H I gas in absorption towards the central regions of radio galaxies

5TH WORKSHOP ON CSS AND GPS RADIO SOURCES

MAY 27-29, 2015, RIMINI, ITALY

Yogesh Chandola

NAOC, CAS, Beijing, China

yogesh.chandola@gmail.com, yogesh.chandola@bao.ac.cn

May 29, 2015

Collaborators

D. J. Saikia
NCRA-TIFR, Pune, India
Cotten College State University, Guwahati, India

Neeraj Gupta
IUCAA, Pune, India

S.K. Sirothia
NCRA-TIFR, Pune, India
Rhodes University, South Africa

C. J. Salter, Tapasi Ghosh, Robert Minchin
Arecibo observatory, Puerto Rico, Arecibo, USA

Outline

21-cm associated HI absorption towards radio sources

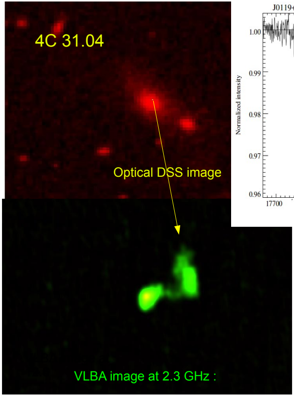

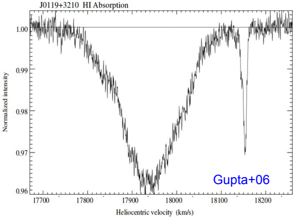

- **ISM : Cold neutral medium (molecular, atomic), Warm neutral medium, H II, Hot ionized medium, dust, stars.**
- **HI : Diffuse cold neutral medium, 21 cm, transition between two hyperfine energy level** 1

- Emission: Global HI properties, detection depends on HI content, sensitivity issues.
- Absorption: Mainly depends on strength of background source , different line profiles (symmetric, blue-shifted, red-shifted), line width (broad and narrow), integrated optical depth.
- Observations at different spatial and spectral resolution and sensitivities.

- **Why to study cold gas (HI) kinematics and distribution ? Triggering and fueling of radio AGN activity (Talk by Fillipo Maccagni), Radio source evolution, Feedback from central engine (Next session: Allison's, Rafaella's talk), AGN unification scheme (Gupta & Saikia 06).**

HI gas properties in compact radio sources of different luminosities

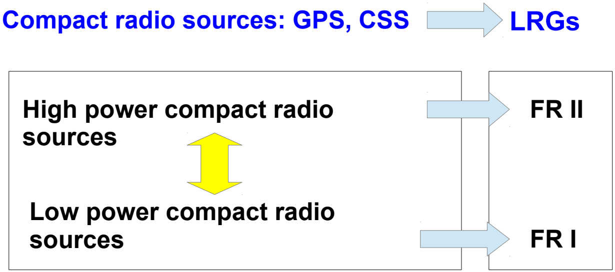

- **Differences in HI gas properties (Detection rate, column densities, relative velocity) with luminosities. Why interesting ?**
- Triggering and fueling of radio AGN activity: Mergers, interactions, bars, Accretion of hot halo gas related with low luminosity radio sources ; Dichotomy in compact radio sources (LERGs, HERGs; Different accretion mode) **(Best & Heckman 2014)**
- Radio source evolution (An & Baan 2012), Talk by Kunert-Bazraszewska.

HI gas properties in compact radio sources of different luminosities

- HI studies towards low luminosity compact nearby radio sources, in order to compare properties of HI gas associated with different luminosity radio sources at early stage of radio source evolution. **Chandola, Sirothia & Saikia, 2011, MNRAS, 418, 1787**
- Sample of 18 sources known as CORALz (**CO**mpact **RA**dio sources **A**t **L**ow red-shift) core sample **(Snellen et al. 2004)**: $S_{1.4GHz}$>100mJy, Angular size $<$ 2 arcsec, Red-shift range 0.024-0.152, $\sim$100 times weaker than those studied by **Gupta et al. 2006**.
- GMRT observations during Dec. 2009 - Feb. 2010, Baseband Bandwidth 4 MHz ($\sim$ 900 km/s), Spectral channels 128 (velocity resolution $\sim$ 7 km/s).

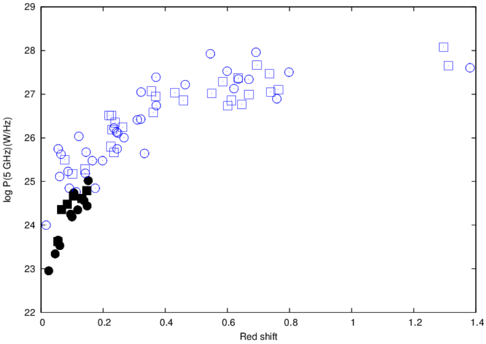

HI absorption detection rates in different luminosity sources

- **High luminosity compact radio sources** (Pihlström et al. 2003, Vermeulen et al. 2003, Gupta et al. 2006):
  HI absorption studies towards have reported higher detection rate towards GPS sources (∼50%) than CSS sources (∼33%).
- **Low luminosity compact radio sources**
  Chandola et al. 2011 :
  HI absorption detections towards 7/17 (41 %) sources.
  Higher detection rate towards (3/6) GPS sources than (4/11) CSS sources.
  Gereb et al. 2015 : WSRT observations 6/11 (54 %) CORALZ ; 4/8 common with our observations [2 new detections (J083637+440110 & J143521+505123), 1 new blue-shifted component (J1602+5243)]
- **The column densities range:** $\sim \mathbf{1.78 \times 10^{20}}$ **to** $\mathbf{10^{22}}$ $\mathbf{cm^{-2}}$
  Median value of $\sim\mathbf{7{\times}10^{20}cm^{-2}}$**.**
  The more luminous GPS & CSS objects the median value is $\sim\mathbf{5{\times}10^{20}cm^{-2}}$.
- **The upper limits for non-detections range from** $\sim$**0.9 to** $\sim$ **4.2** $\mathbf{\times10^{20}cm^{-2}}$.

Results:detections

J150805+342323

- ΔI_{rms}=0.95 mJy/beam/ch, I_c = 134 mJy, τ_{rms} =0.007, N(HI)=125$\times 10^{20}$ cm^{-2}
  z= 0.0456, Three blue shifted components possibly due to jet-cloud interactions

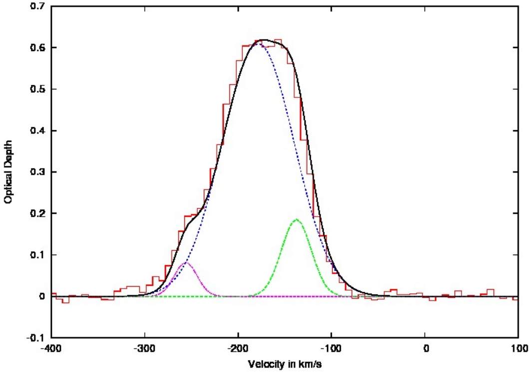

Figure: HI spectra towards J150805+342323Chandola, Sirothia & Saikia, 2011, MNRAS, 418, 1787

Results:detections

J150805+342323

- ΔI_{rms}=0.95 mJy/beam/ch, I_c = 134 mJy, τ_{rms} =0.007, N(HI)=125×10^{20} cm^{-2}
  z= 0.0456, Three blue shifted components possibly due to jet-cloud interactions

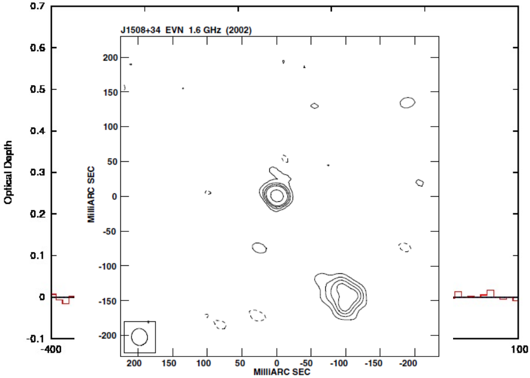

Figure: HI spectra towards J150805+342323Chandola, Sirothia & Saikia, 2011, MNRAS, 418, 1787
Figure: J150805+342323 EVN map (1.6 GHz)de Vries N. et al., 2009, A&A, 498, 641

HI column density vs. linear size

- Anti-correlation between HI column density & linear size (Pihlström et al. 2003, Gupta et al. 2006) for higher luminosity CSS & GPS objects is also consistent for lower luminosity radio sources.
- Pihlström et al. 2003: radial density profile with a disk geometry; Curran et al. 2013: N(HI) derived from $\tau_{obs} \propto f \propto 1/d_{em}$.
- Gereb et al. 2015: No correlation from their sample.

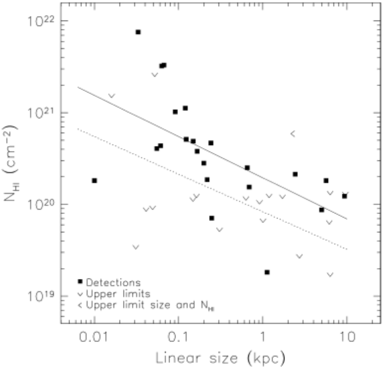

Figure: ■ **Detections** ; ∨ **Upper limits**; < **Upper limits size & N(HI)**
Pihlström Y. M., Conway J. E., Vermeulen R. C., 2003, A&A, 404, 871

HI column density vs. linear size

- Anti-correlation between HI column density & linear size (Pihlström et al. 2003, Gupta et al. 2006) for higher luminosity CSS & GPS objects is also consistent for lower luminosity radio sources.
- Pihlström et al. 2003: radial density profile with a disk geometry; Curran et al. 2013: N(HI) derived from $\tau_{obs} \propto f \propto 1/d_{em}$.
- Gereb et al. 2015: No correlation from their sample.

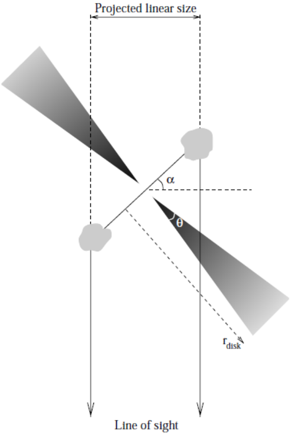

Figure: Cartoon of the CSS/GPS geometry used for the disk modelling
Pihlström Y. M., Conway J. E., Vermeulen R. C., 2003, A&A, 404, 871

HI column density vs. linear size

- Anti-correlation between HI column density & linear size (Pihlström et al. 2003, Gupta et al. 2006) for higher luminosity CSS & GPS objects is also consistent for lower luminosity radio sources.
- Pihlström et al. 2003: radial density profile with a disk geometry; Curran et al. 2013: N(HI) derived from $\tau_{obs} \propto f \propto 1/d_{em}$.
- Gereb et al. 2015: No correlation from their sample.

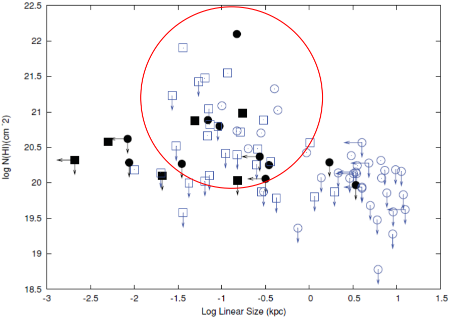

Figure: ⊡ ⊙ **from Gupta et al. 2006;■ • our observations**; circles: CSS objects; squares: GPS objects ; arrows denote upper limits
Chandola, Sirothia & Saikia, 2011, MNRAS, 418, 1787

Velocity w.r.t optical systemic velocity

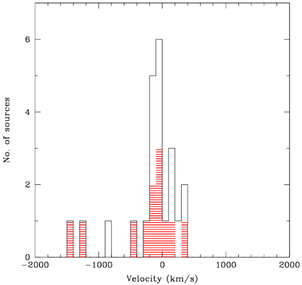

Figure: Histogram from Gupta et al. (2006) shows velocity distribution for high luminosity CSS & GPS (shaded) objects
Gupta N., et al., 2006, MNRAS, 373, 972

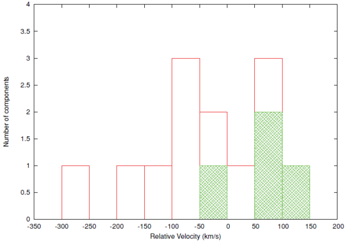

Figure: Histogram from Chandola et al. (2011) shows velocity distribution for low luminosity CSS & GPS (shaded) objects
Chandola, Sirothia & Saikia, 2011, MNRAS, 418, 1787

Although the number of lower luminosity sources need to be increased, present observations suggests that low velocity blue-shifted feature could be due to low power jets.

Differences in circumnuclear HI gas properties of compact and large radio sources

- To get a better understanding of this, we need to have observation for HI absorption towards cores of larger radio sources with resolution probing similar length scales as of compact radio sources with similar optical depth sensitivities.

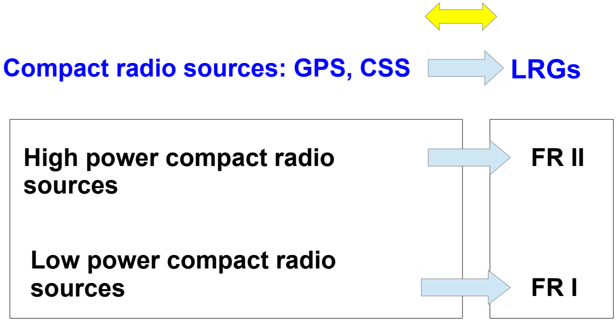

Differences in circumnuclear HI gas properties of compact and large radio sources

- To get a better understanding of this, we need to have observation for HI absorption towards cores of larger radio sources with resolution probing similar length scales as of compact radio sources with similar optical depth sensitivities.

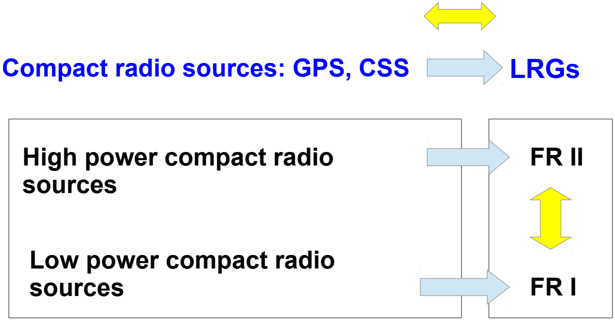

Sample and observation

- **Chandola, Gupta & Saikia, 2013, MNRAS, 429, 2380** have reported H I absorption studies towards the cores of larger radio sources.
  - to understand evolution in H I gas properties with radio source evolution.
  - to look for, if there are any differences in detection rates for FR I & FR II radio sources.

- We compiled a sample of 16 large radio sources (10 FR I & 6 FR II) from 3CR & B2 catalogue with following criteria:
  - Core flux density at 1.4 GHz $>$ 100 mJy.
  - Radio structure is such that core emission can be distinguished from extended bridge emission with spatial resolution of a few arsec or better.
  - Red-shifted 21-cm absorption should be within GMRT observing band ($0.016 < z < 0.134$).
- We observed these sources with the GMRT in two phases 2004-2006 & 2009-2010 with following specifications:
  - BB BW =4 MHz ; 128 channels.
  - velocity resolution $\sim$7 km/s.
  - Total observing time with calibration overheads $\sim$ 8 hrs.
  - The standard flux density(bandpass calibrators) 3C 286, 3C147 & 3C 48 were observed usually every 3 hrs.

Sample and observation

- In order to increase our sample of large radio sources, we also added sources from literature (van Gorkom et al. (1989), Morganti et al.(2001) & Emonts et al. (2010), which satisfied criteria listed below:
  - Largest Linear Size > 15 kpc.
  -Spatial resolution such that it corresponds to < 15 kpc for our red-shift range.
  - Avoided inclusion of QSOs, BL Lacs, Spirals or Seyferts in the sample.
  - Excluded the sources which were reported with 'only detections', as it would have impact on our statistical analysis[1].
- Combining '16 sources' from our observations with '31 sources' from literature form our 'cores sample' of 47 sources which we used for our statistical studies.

[1] However we did use additional '9 sources' with arcsec resolution reported with 'only detection ' for other studies.

Results: detection

- From our observations of 16 sources, we have HI absorption detection towards only one FR II source 3C 452 (Gupta & Saikia 2006).
- Out of 10 FR I sources we have detections towards none, while out of 6 FR II sources we have detection towards 1.

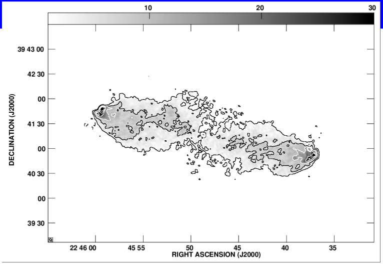

Figure: 3C 452 map from Gupta & Saikia (2006)
Gupta N.& Saikia D.J., 2006, MNRAS, 370L, 80

3C 452

- z = 0.0811 ; FR II source; LAS=256" LLS =386 kpc
- **Map**
  - rms noise = 0.3 mJy/beam
  - Peak flux density (core)=194 mJy/beam
  - Beam : 2.89"×2.24" ; P.A. : -70°
  - Contours: 2.5 × (-1, 1, 2, 4, 8, 16, 32, 64) mJy/beam
- **HI absorption spectra**
  - ΔI_{rms}=1.00 mJy/beam/channel
  - τ_{rms}=0.058 /beam/channel
  - N(HI)= 6.39 $\times 10^{20}$cm^{-2}
  - v_{sys}(optical)=24313 kms^{-1}

Results: detection

- From our observations of 16 sources, we have HI absorption detection towards only one FR II source 3C 452 (Gupta & Saikia 2006).
- Out of 10 FR I sources we have detections towards none, while out of 6 FR II sources we have detection towards 1.

3C 452

- $z = 0.0811$; FR II source; LAS=256" LLS =386 kpc
- **Map**
  - rms noise = 0.3 mJy/beam
  - Peak flux density (core)=194 mJy/beam
  - Beam : 2.89"×2.24" ; P.A. : -70°
  - Contours: 2.5 × (-1, 1, 2, 4, 8, 16, 32, 64) mJy/beam
- **HI absorption spectra**
  - ΔI_{rms}=1.00 mJy/beam/channel
  - τ_{rms}=0.058 /beam/channel
  - N(HI)= 6.39 $\times 10^{20}$cm^{-2}
  - v_{sys}(optical)=24313 kms^{-1}

Figure:
Gupta N.&
)

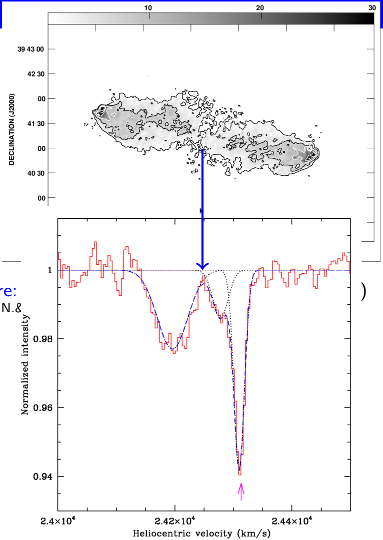

Figure: HI spectra towards core of 3C 452 from Gupta & Saikia (2006)
Gupta N.& Saikia D.J., 2006, MNRAS, 370L, 80

HI absorption detection rate

The column densities or upper limits to these sources in our 'cores sample' range from $\sim 0.5\times10^{20}$ to $69\times10^{20}\,\mathrm{cm}^{-2}$. The median column density sensitivity of our 'cores sample' including the upper limits is $3.1\times10^{20}\,\mathrm{cm}^{-2}$.

- The detection rate for cores sample is rather low (7/47 ; ∼15 %) as compared with the detection rate for compact CSS & GPS sources (28/49; ∼ 57 %). For the entire 'CSS & GPS' sample this rate is (31/84; ∼ 37%). This suggests that there is evolution in circumnuclear gas properties with the radio source evolution.
- HI is detected in absorption towards 4/32 (∼13 %) FR I objects, compared with 3/15(∼20 %) for the FR II sources.

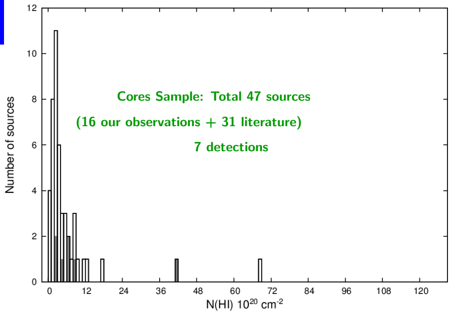

Figure: Chandola, Gupta & Saikia, 2013, MNRAS,429, 2380

HI absorption detection rate

The column densities or upper limits to these sources in our 'cores sample' range from $\sim 0.5 \times 10^{20}$ to 69×10^{20} cm^{-2}. The median column density sensitivity of our 'cores sample' including the upper limits is 3.1×10^{20} cm^{-2}.

- The detection rate for cores sample is rather low (7/47 ; ∼15 %) as compared with the detection rate for compact CSS & GPS sources (28/49; ∼ 57 %). For the entire 'CSS & GPS' sample this rate is (31/84; ∼ 37%). This suggests that there is evolution in circumnuclear gas properties with the radio source evolution.
- HI is detected in absorption towards 4/32 (∼13 %) FR I objects, compared with 3/15(∼20 %) for the FR II sources.

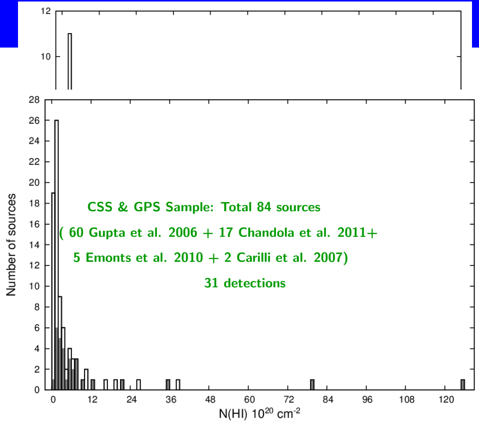

Figure: Chandola, Gupta & Saikia, 2013, MNRAS, 429, 2380

HI absorption detection rate

The column densities or upper limits to these sources in our 'cores sample' range from $\sim 0.5\times10^{20}$ to $69\times10^{20}\mathrm{cm}^{-2}$. The median column density sensitivity of our 'cores sample' including the upper limits is $3.1\times10^{20}\mathrm{cm}^{-2}$.

- **The detection rate for cores sample is rather low (7/47 ; $\sim$15 %) as compared with the detection rate for compact CSS & GPS sources (28/49; $\sim$ 57 %). For the entire 'CSS & GPS' sample this rate is (31/84; $\sim$ 37%). This suggests that there is evolution in circumnuclear gas properties with the radio source evolution.**
- **HI is detected in absorption towards 4/32 ($\sim$13 %) FR I objects, compared with 3/15($\sim$20 %) for the FR II sources.**

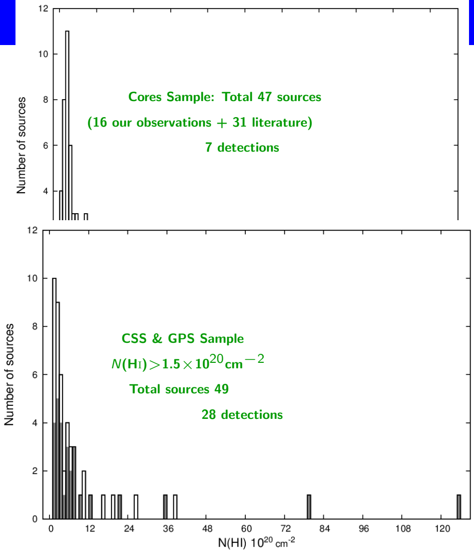

Figure: Chandola, Gupta & Saikia, 2013, MNRAS, 429, 2380

Relative velocity of absorbing gas

- Relative velocity for 16 detections (7 from cores sample & 9 additional detections not included in 'cores sample') was compared to 33 detections (31 from 'CSS & GPS' sample & 2 additional compact source detection not included in the statistical sample).
- We do not find any significant difference between the two except for a few CSS and GPS objects have a large blue-shifted velocities of $\gtrsim$ 1000 kms^{-1}.
- The highly red-shifted component seen towards the core of NGC 1275 in the Perseus cluster could be due to a gas cloud or galaxy in the intracluster medium moving towards NGC 1275.

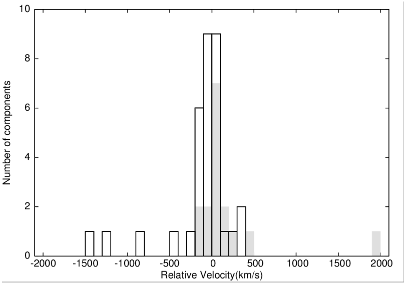

Figure: Shades : Large Radio Sources; Boxes : Compact radio sources Chandola, Gupta & Saikia, 2013, MNRAS, 429, 2380

Fueling of rejuvenated radio sources & HI gas

Is there any relation between rejuvenation activity and HI gas ? Evidences of HI gas towards rejuvenated radio source.

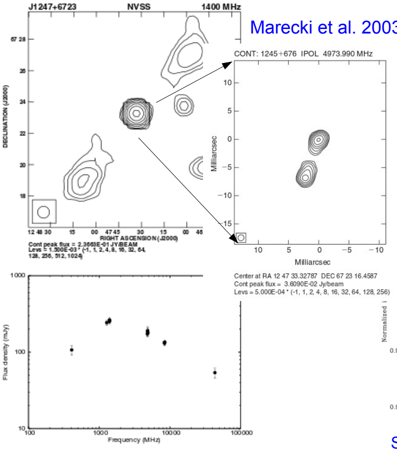

Marecki et al. 2003

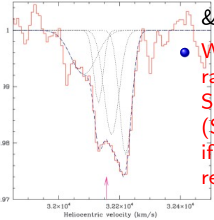

Saikia, Konar, Gupta (2007)

- Examples of earlier HI absorption studies towards rejuvenated radio sources
  - the inner double of the DDRG, J1247+6723 (Saikia, Gupta & Konar 2007); 3C236 (Schilizzi et al. 2001); 3C293 (Beswick, Pedlar & Holloway 2002)
- We studied HI absorption towards radio sources 4C 29.30 (Chandola, Saikia, Gupta, 2010), and CTA 21 (Salter et al. 2010) in order to see if there is any relation between rejuvenation activity and HI gas.

4C 29.30 morphology

VLA D-array image overlayed over DSS image; first contour 0.3 mJy/beam

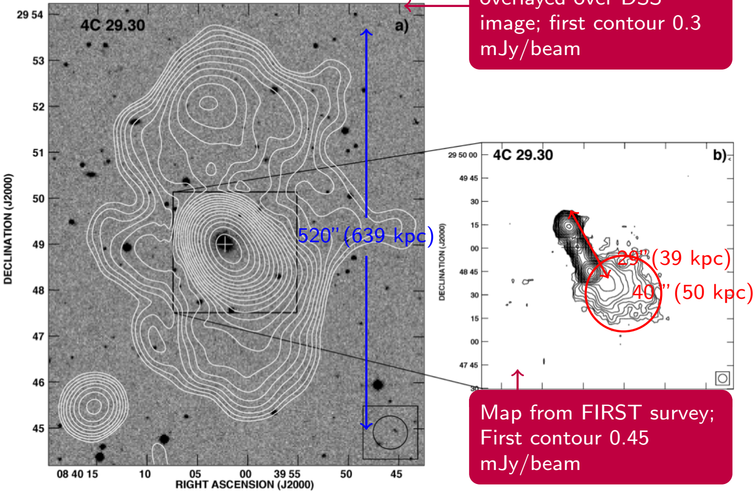

Map from FIRST survey; First contour 0.45 mJy/beam

Figure: Collage reproduced from Jamrozy et al. 2007

HI absorption towards core of 4C 29.30

Chandola Y., Saikia D.J., Gupta N., 2010, MNRAS 403, 269

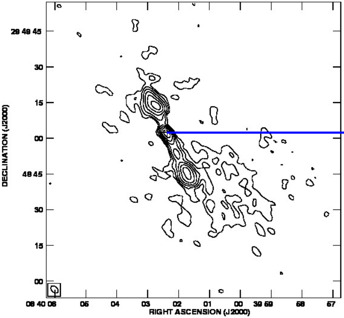

Figure: GMRT map at 1332 MHz from Chandola, Saikia & Gupta (2010)

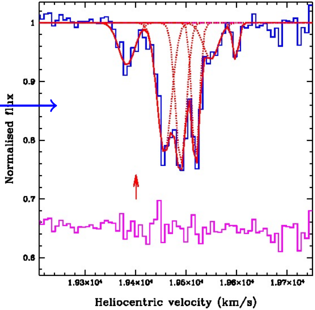

Figure: HI absorption spectra towards the 4C 29.30 core Chandola, Saikia & Gupta (2010)

Beam: 3.60" ×2.35"; P.A.: 45.7°
I_{peak}(core): 78.9 mJy/beam
r.m.s noise: 0.4 mJy/beam

z= 0.0647;
ΔI_{rms}∼1 mJy/beam/chan.
N(HI)(core)=4.7×10^{21}cm^{-2}

CTA 21 morphology

CTA 21 is a candidate rejuvenated radio source.

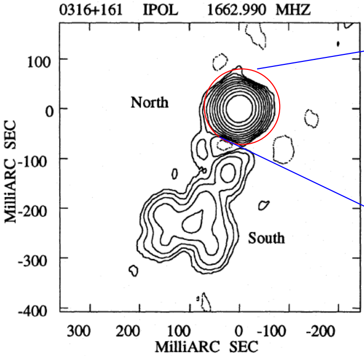

Fig. 3. Tapered MERLIN + VLBI image restored with a 40 mas circular beam. Contour levels are –5, 5, 10, 20, 40, 80, 150, 300, 600, 1250, 2500 times the noise of 0.75 mJy/beam. The peak flux density is 5908 mJy/beam

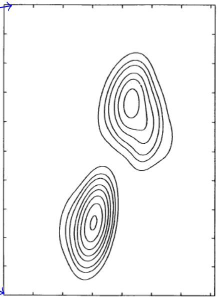

FIG. 2.—Hybrid map of CTA 21 at 6 cm. The contours are at 5%, 10%, 15%, 25%, 35%, 50%, 70%, and 95% of the peak, which equals 722 mJy per beam area or a brightness temperature of 3.77×10^9 K. The tick marks along the borders are 2.8 milli-arcsec apart, and the total flux density of the clean components is 3.19 Jy. The size of the clean beam is 5 by 2 milli-arcsec, with the major axis in a position angle of $-10°$.

Figure: MERLIN+VLBI image at 1663 MHz from **Dallacasa et al. 1995, A&A, 295, 27**; angular res. ∼40 mas

Figure: VLBI map at 4831 MHz from **Jones D, 1984, ApJ, 276, L5** ; angular size 12 mas

Salter C.J., Saikia D.J., Ghosh T., Minchin R., Chandola Y., 2010, ApJ, 715, L117
We discovered new 21cm HI absorption towards CTA 21 with the Arecibo telescope.

CTA 21cm observation

- Arecibo Observation : June 2009
- **Red-shift** of strongest component 0.9057 agrees with the optical red-shift (Labiano et al. 2007)
- Velocity resolution : 16.1 km/s Frac. ab. rms =0.00055
- Total $N(\mathrm{HI}) = 7.92 \times 10^{20} \mathrm{cm}^{-2}$

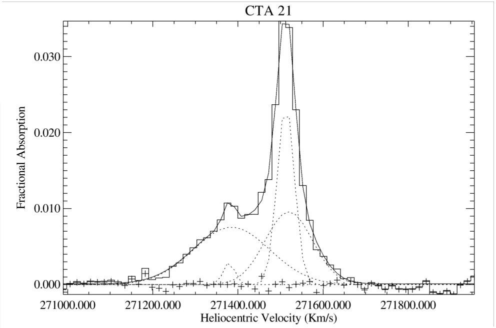

Figure: Fractional absorption vs. Heliocentric Velocity (Salter et al. 2010)

Summary and future work

- We detected new HI absorption towards towards CTA 21 and 7 sources from CORALz sample.
- HI gas properties do not show any significant difference in low & high luminosity compact radio sources.

  Follow up

  - Large scale HI gas in emission towards 7 sources with HI absorption.

  - High resolution VLBI observations to know precisely the location of absorbing gas.

  Future

  - New samples of low luminosity radio sources; Upcoming telescopes like SKA, LOFAR with better sensitivity and resolution helpful.
- Significantly low HI absorption detections towards cores of larger radio sources as compared to compact radio sources suggests evolution in circumnuclear gas properties with radio source evolution.

  - Larger samples of brighter core radio sources; better sensitivity observations for fainter core $<$ 100 mJy (Recent work by Gereb et al. 2015).

  - Stacking technique to get idea of statistics (e.g. Géreb et al. 2015)
- HI absorption towards 4C 29.30, and CTA 21 shows evidence for increasing trend of detection of HI gas and rejuvenation activity.

  - Reverse search for extended emission in GPS with HI absorption detected (GMRT 310 MHz data on 7 GPS sources from Gupta et al. 06).
- Higher red-shifts; lesser known sources and lesser detections; increase in number of sources with techniques like USS and IRFS; surveys such as FLASH with ASKAP in near future.

Thank you !!!